

Inhibition of Cell Migration and Cell Division Correlates with Distinct Effects of Microtubule Inhibiting Drugs*[§]

Received for publication, July 2, 2010, and in revised form, August 3, 2010. Published, JBC Papers in Press, August 9, 2010, DOI 10.1074/jbc.M110.160820

Hailing Yang¹, Anutosh Ganguly¹, and Fernando Cabral²

From the Department of Integrative Biology and Pharmacology, University of Texas Medical School, Houston, Texas 77030

Drugs that target microtubules are thought to inhibit cell division and cell migration by suppressing dynamic instability, a “search and capture” behavior that allows microtubules to probe their environment. Here, we report that subtoxic drug concentrations are sufficient to inhibit plus-end microtubule dynamic instability and cell migration without affecting cell division or microtubule assembly. The higher drug concentrations needed to inhibit cell division act through a novel mechanism that generates microtubule fragments by stimulating microtubule minus-end detachment from their organizing centers. The frequency of microtubule detachment in untreated cells increases at prophase suggesting that it is a regulated cellular process important for spindle assembly and function. We conclude that drugs produce differential dose-dependent effects at microtubule plus and minus-ends to inhibit different microtubule-mediated functions.

Microtubules are essential cytoskeletal structures that have been implicated in many important cellular processes including vesicle transport, cell structure and motility, signaling, and cell division. They appear as small hollow tubes whose walls are composed of protofilaments assembled from the head-to-tail addition of $\alpha\beta$ -tubulin heterodimers. This ordered assembly generates polar microtubules that are arranged with their minus-ends embedded in nucleating centers, called centrosomes, located near the nuclear membrane, and with their plus-ends extended out toward the cell periphery. Microtubules are highly dynamic filaments that exhibit a behavior called dynamic instability (1). Microtubules engaged in dynamic instability experience stochastic episodes of growth and shortening of their plus-ends interspersed with variable periods of pause during which there is no net change in length.

Because microtubules are essential for assembly and function of the mitotic spindle apparatus, drugs that bind tubulin inhibit chromosome segregation and block cell division. These toxic effects have led to the widespread use of these agents in the treatment of cancer. For example, the microtubule inhibitors (MIs)³ vinblastine and vincristine have been used since the

1960s and remain first line drugs for the treatment of lymphoma, leukemia, and testicular carcinoma. More recently, taxanes such as paclitaxel have been shown to be very effective against breast and ovarian carcinoma, nonsmall cell lung carcinoma, head and neck tumors, Kaposi’s sarcoma, and others. Although all of these drugs are effective in blocking cell division, they have differing effects on microtubule assembly. One group of MIs that includes vinca alkaloids, colchicine, and colcemid disrupts assembly and causes a depletion of cellular microtubules. A second group that includes taxanes and epothilones promotes assembly and causes increased microtubule density and bundling in treated cells. Despite these differences, both groups of drugs inhibit the normal progression of cells through mitosis.

In addition to their well known effects on cell division, MIs also interfere with cell migration (2, 3). Currently it is unclear whether drug effects on cell migration and mitosis are mediated by a common mechanism. A number of studies have indicated that virtually all MIs inhibit mitosis by suppressing microtubule plus-end dynamics (4), and alteration of dynamics has been used to explain drug inhibition of cell migration as well (5). On the other hand, there is evidence that the drug concentrations affecting migration can be lower than those that affect mitosis, suggesting that different mechanisms may be involved (6). In the studies described here, we examined the effects of MIs on microtubule dynamic instability, microtubule assembly, cell division, and cell migration. We report that low drug concentrations suppress both dynamic instability and cell migration, but higher drug concentrations are needed to inhibit microtubule assembly and cell division. The effects of the higher drug concentrations are mediated by a novel mechanism affecting the stability of microtubule minus-end attachment to centrosomes and spindle poles.

EXPERIMENTAL PROCEDURES

Cell Lines, Antibodies, and Drugs—Chinese hamster ovary (CHO), CHO mutants CV 2-8 (7), Tax 5-6 (8), MCF-7, and COS-7 cells were all maintained in α -minimum Eagle’s medium (Mediatech, Inc., Manassas, VA) supplemented with 5% fetal bovine serum (Gemini Bio-Products, West Sacramento, CA). PTK2 cells were maintained in F10 medium (Thermo Scientific, Logan, UT) containing 10% fetal bovine serum. Ishikawa cells were maintained in DMEM (Invitrogen) with 10% fetal bovine serum. Drugs and mouse monoclonal antibody DM1A to α -tubulin were from Sigma, and goat anti-mouse IgG conjugated to Alexa 488 or Alexa 647 was purchased from Invitrogen. Antibodies were used at a concentration of

* This work was supported, in whole or in part, by National Institutes of Health Grant CA85935 (to F. C.).

[§] The on-line version of this article (available at <http://www.jbc.org>) contains supplemental Tables S1 and S2, Figs. S1–S5, and Movies 1 and 2.

¹ Both authors contributed equally to this work.

² To whom correspondence should be addressed: Dept. of Integrative Biology and Pharmacology, The University of Texas Medical School, 6431 Fannin St., Houston, TX 77030. Tel.: 713-500-7485; Fax: 713-500-7456; E-mail: fernando.r.cabral@uth.tmc.edu.

³ The abbreviation used is: MI, microtubule inhibitor.

1:100 for immunofluorescence and 1:2000 for Western blots unless otherwise stated.

Colony Formation Assay—Approximately 100 cells were seeded into each of 9 replicate wells in a 24-well dish in the presence of increasing concentrations of drug. Depending on the cell line, cells were allowed to grow 7–12 days until colonies visible to the naked eye were formed. The cells were then stained with 0.05% aqueous methylene blue and photographed as previously described (9). In some cases, quantification was carried out by eluting the dye in 1% SDS and measuring the optical density at 630 nm (10).

Transfection and Live Cell Microscopy—For live cell microscopy cells were seeded onto glass coverslips, grown overnight, and transfected with EGFP-MAP4 (11) using Lipofectamine (Invitrogen). After transfection, the cells were grown 16–48 h and then transferred to McCoy's 5A medium containing 25 mM HEPES (Mediatech). Images were captured 5 s apart using a DeltaVision Core imaging system (Applied Precision, Inc., Issaquah, WA) at 37 °C equipped with a CCD camera and imaging software supplied by the vendor.

Immunofluorescence—Cells were seeded onto glass coverslips, grown to 50–70% confluence, rinsed in PBS, and fixed in methanol at –20 °C for 20 min. To minimize background fluorescence and enhance contrast, cells were sometimes pre-extracted before fixation by incubating them for 1 min at 4 °C with microtubule buffer (20 mM Tris-HCl (pH 6.8), 1 mM MgCl₂, 2 mM EGTA, 0.5% Nonidet P-40) containing 4 μg/ml paclitaxel. Fixed cells were washed in PBS, incubated with DM1A for 1 h at 37 °C, washed again in PBS, and incubated with goat antimouse IgG that included 1 μg/ml 4', 6-diamidino-2-phenylindole (DAPI). Cells were viewed using an Optiphot microscope (Nikon, Inc., Melville, NY) equipped with a MagnaFire digital camera (Optronics, Goleta, CA).

Cell Migration Assay—Cells were seeded uniformly into 6-well dishes and grown to 80% confluence. A scratch was made through the center of each well using a wooden toothpick, floating cells were removed, and the cells were allowed to recover for 2 h. Fresh media containing increasing drug concentrations were then added. The dish was incubated at 37 °C in a Pathway bioimaging system (BD Biosciences) for 30 min before acquiring images. The wound in the cell monolayer was photographed every 15 min using a 10× objective. For the first image in a time sequence, the distance between the edges at 10 separate locations was averaged. Similar averages were then calculated at each subsequent time point using the same ten locations, and the distance the cells migrated was calculated as the change in the distance between edges of the wound divided by two. This experiment was repeated four times, averaged for each time point, and plotted against time to calculate the rate of migration.

Measurement of Polymerized and Free Tubulin—To measure the fraction of tubulin assembled into microtubules, cells grown 16 h with or without MIs were lysed in 200 μl of microtubule buffer containing 0.14 M NaCl and 4 μg/ml paclitaxel to keep the polymerized microtubules intact (12). The lysates were centrifuged at 12,000 × *g* for 10 min at 4 °C. An equal amount of bacterial cell lysate containing glutathione *S*-transferase- α -tubulin was added to each supernatant and pellet frac-

tion to monitor possible losses of material during subsequent steps. Proteins were precipitated with acetone, dissolved in SDS sample buffer, and analyzed by Western blots as previously described (10). Tubulin was detected and quantified on the Western blots stained with DM1A antibody and Alexa 647-conjugated goat antimouse IgG using a Storm 860 scanner equipped with an infrared filter (GE Healthcare). The percent of total tubulin polymerized into microtubules was calculated by normalizing tubulin in the supernatant and pellet fractions to the amount of glutathione *S*-transferase- α -tubulin, dividing the normalized value from the pellet by the sum of the values from supernatant and pellet and multiplying the quotient by 100. An average value \pm S.D. from six experiments was calculated at each drug concentration.

Calculation of Microtubule Dynamics—The lengths of individual microtubules labeled by EGFP-MAP4 were measured using ImageJ software and plotted as a function of time to generate microtubule life histories. The rates of growth and shortening were calculated from the slopes of each curve using linear regression. If the change of length in a microtubule between two time points was greater than 0.5 μm, it was considered real growth or shortening. Otherwise, it was considered to be a pause. The frequency of catastrophe, a transition from either growth or pause to a shortening phase, was calculated as the number of catastrophes divided by the total time spent in growth and pause states. The frequency of rescue, a transition from shortening to either growth or pause states, was calculated as the number of rescues divided by the total time spent in shortening phases. Dynamicity, an overall parameter used to characterize the degree of microtubule dynamic instability, was calculated by dividing the total of all the changes in length during growth and shortening phases by the total time the microtubule was observed. Only microtubules persisting for more than 2 min were included in calculations of catastrophe, rescue, and dynamicity. Each parameter is represented as the mean \pm S.E. Student's *t* test was utilized to compare drug-treated cell lines to untreated controls. Differences with *p* < 0.05 were considered significant.

RESULTS

Effect of MIs on Microtubule Organization and Cell Division—We used a colony formation assay to determine the lowest drug concentration needed to inhibit CHO cell proliferation and found that reductions in colony size and numbers began to appear at ~25 nM colcemid or 15 nM vinblastine (supplemental Fig. S1). To assess the effects on microtubules, cells were treated with drugs for 2 days and viewed by tubulin immunofluorescence (Fig. 1). As expected, drug concentrations below those needed to inhibit colony formation had little or no effect on microtubule density or organization. In addition, almost all the cells were normal in size and had single, mostly symmetrical nuclei that indicated they had undergone normal cell division (Fig. 1, *A*, *B*, and *E*). Consistent with normal cell division, metaphase spindles with a normal appearance were present (Fig. 1, upper insets). At 25 nM colcemid or 15 nM vinblastine, however, the cell populations became heterogeneous. Although most cells exhibited apparently normal cytoplasmic microtubule arrays, many had multiple or oddly shaped nuclei indicating

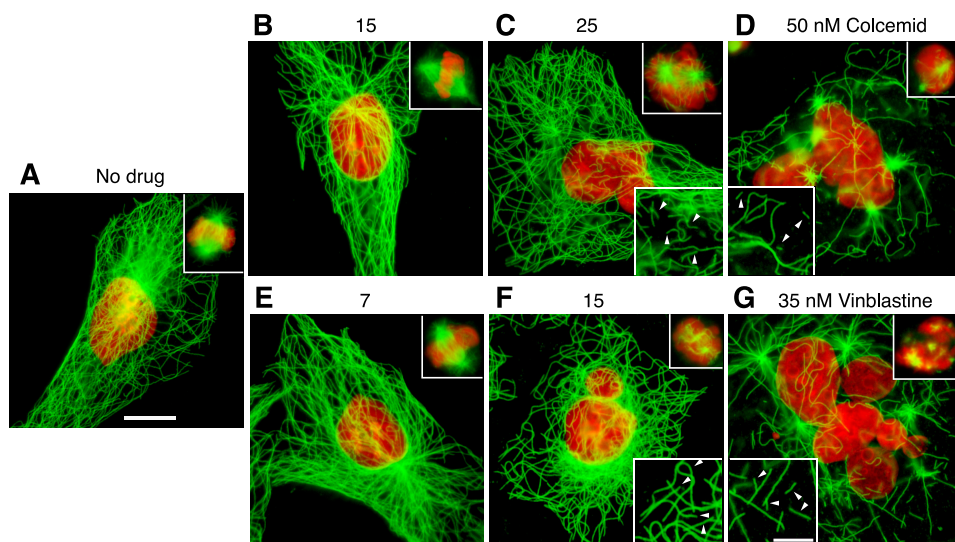


FIGURE 1. **Tubulin immunofluorescence.** CHO cells were treated for 2 days with the indicated concentrations of colcemid or vinblastine and stained with DM1A for tubulin (green) and DAPI for DNA (red). Bar = 10 μm . Upper insets show representative mitotic cells at each of the indicated drug concentrations. Lower insets show 1.5-fold enlargements of a part of the cell to more clearly indicate the presence of microtubule fragments (arrowheads); bar = 5 μm .

that they had experienced problems in chromosome segregation and cell division (Fig. 1, C and F). In addition, mitotic cells in a prometaphase-like state with disorganized chromosomes and spindle microtubules became abundant (see upper insets). At still higher drug concentrations (Fig. 1, D and G), cytoplasmic microtubules were obviously disrupted, and the cells were large and extensively multinucleated, indicating that they had experienced severe problems in chromosome segregation and re-entered G_1 phase without dividing. Similar changes have previously been described for this cell line when treated with drugs or when harboring mutations that affect spindle function (13–15).

Low Concentrations of MIs Suppress Microtubule Dynamics but Not Mitosis—Previous studies have indicated that MIs inhibit mitosis by suppressing microtubule dynamic instability (4). To test this mechanism, we transfected CHO cells with EGFP-MAP4 and used live cell imaging to directly measure drug effects on microtubule plus-end dynamics. MAP4 is a microtubule-associated protein that decorates microtubules but has no effect on microtubule assembly or drug sensitivity when overexpressed or inhibited (16, 17). Moreover, we recently used photobleaching to show that MAP4 residence time on microtubules is very short (half-life <5 s),⁴ a finding that is inconsistent with a structural role for MAP4 in microtubule stability. By measuring microtubule length as a function of time, we generated life-history plots that were used to calculate various dynamic parameters including growth rates and durations, shortening rates and durations, transitions from growth or pause to shortening (catastrophes), transitions from shortening to growth or pause (rescues), and the total distance of growth plus shortening per unit time during the period of observation (dynamicity). The parameters that we calculated for vinblastine and colcemid at a series of drug concentrations

are summarized in supplemental Tables S1 and S2. It should be noted that the parameters for untreated CHO cells were very similar to published values from studies in which microinjection of rhodamine-labeled tubulin was used to create fluorescent microtubules (18). Thus, our methodology produced data that agree well with the data produced by other approaches for measuring microtubule dynamics and has the advantage that the fluorescent reporter is not incorporated into the microtubule lattice. Also in agreement with previous studies (4), the data summarized in supplemental Tables S1 and S2 demonstrate that treatment with vinblastine or colcemid decreased many of the parameters associated with dynamic instability including growth rates, shortening rates, and dynamicity.

The frequency of catastrophe remained mostly unchanged, the frequency of rescue increased by 35–50%, and the time spent in a paused state increased almost 60%. Overall, the microtubules in drug-treated cells exhibited smaller excursions of growth and shortening and spent less time in either activity, changes that are collectively best characterized by the parameter called dynamicity.

These effects on dynamic instability were seen at low drug concentrations that were insufficient to inhibit cell division (see supplemental Tables S1 and S2). An example of life history plots generated using the minimum drug concentrations that maximally suppressed microtubule dynamics is shown in Fig. 2. Untreated CHO microtubules exhibited significant periods of growth and shortening (Fig. 2A), but the addition of 7 nM colcemid (Fig. 2B) or 2.5 nM vinblastine (Fig. 2C), concentrations well below those needed to inhibit cell division, strongly suppressed microtubule dynamic behavior. Thus, we agree with the notion that MIs suppress microtubule dynamics, but we found no evidence that the drugs inhibit cell division by this action alone. We reached a similar conclusion from more limited data using PtK2 and MCF-7 cell lines.

Low Drug Concentrations Inhibit Cell Migration—The ability of low drug concentrations to suppress microtubule dynamics without inhibiting cell division led us to question whether these low concentrations would affect other microtubule-mediated functions. Because previous studies indicated that MIs affect cell migration (6), we tested the effects of colcemid and vinblastine on CHO cell movement in a wound healing assay. For these experiments, a scratch mark was introduced into a monolayer of CHO cells, and the rate at which the wound closed was measured. An example of such an experiment is shown in supplemental Fig. S2, and measurements of the distance traveled by each edge of the wound as a function of time are plotted in Fig. 3A. Untreated CHO cells closed the wound at a rate of ~ 22 $\mu\text{m}/\text{h}$ for an average cell velocity at each edge of the wound of

⁴ H. Yang, A. Ganguly, and F. Cabral, unpublished data.

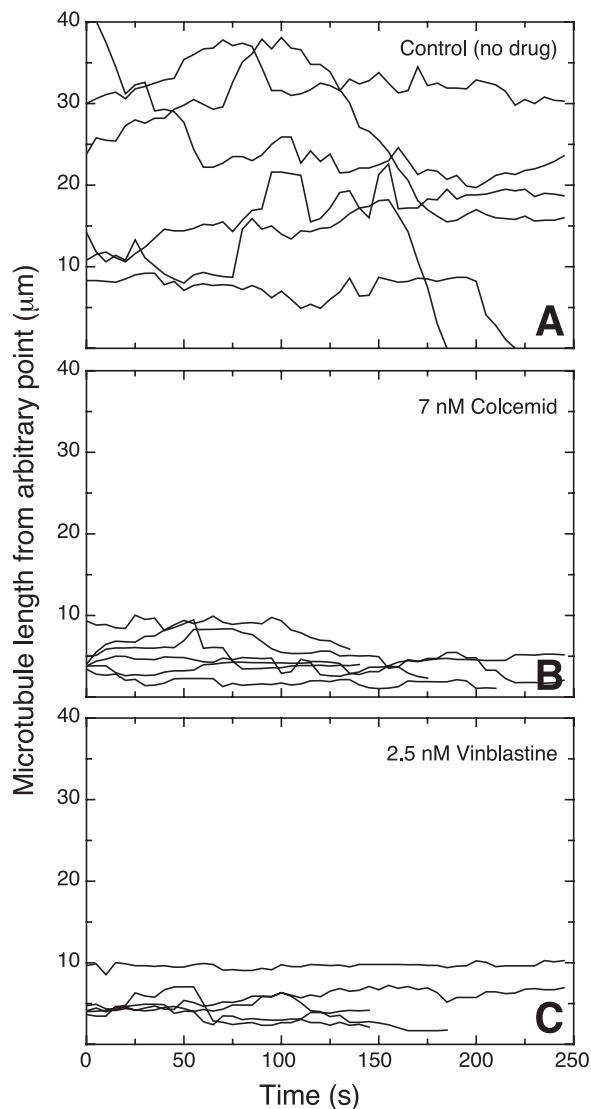


FIGURE 2. **Microtubule life history plots.** CHO cells were transfected with EGFP-MAP4, grown overnight, and examined by time-lapse fluorescence microscopy at 37 °C 30 min after the addition of colcemid or vinblastine. Images were taken every 5 s, and the microtubule length, measured from an arbitrary fixed point, was plotted against time. Each *line* represents a different microtubule. The drug concentrations were chosen to maximally suppress microtubule dynamics without affecting cell division.

11 $\mu\text{m}/\text{h}$. Consistent with a role for microtubule dynamics in cell migration, a gradual dose-dependent decrease in the average cell velocity to 1.8 (colcemid) and 2.4 $\mu\text{m}/\text{h}$ (vinblastine) occurred at concentrations that did not inhibit mitosis (Fig. 3A).

Because the rate of wound healing only measures the average speed at which cells move in the direction of the wound, we also tracked individual cells to determine whether suppressing microtubule dynamics affected the directionality of cell movement. To accomplish this, the coordinates of individual nuclei relative to a fixed imperfection in the dish were plotted at 15-min intervals. The results (Fig. 3B) indicated that untreated control cells moved steadily and predominantly in the direction of the wound. The addition of 4 μM vinblastine did not appear to greatly alter the directionality of movement. Rather, it was the persistence of movement that appeared to be most affected

by suppressed microtubule dynamics. In contrast to the untreated control, the drug-treated cells spent many intervals without any significant movement, and when they did move, the distance traveled was shorter. The velocity of movement for the control cells irrespective of direction was calculated by averaging the velocities for each 15 min interval and was found to be $18.3 \pm 1.6 \mu\text{m}/\text{h}$, a value that is 67% higher than the rate calculated from wound closure that only measured velocity in the direction of the wound. This value compares favorably with previous published values for CHO cell movement (19). The velocity of vinblastine-treated cells, calculated using only those intervals in which the cells actually moved, was found to be $11.8 \pm 1.7 \mu\text{m}/\text{h}$. This velocity is almost 5 times higher than the rate calculated from wound healing and is only 35% lower than the control, implying that the major factor limiting the ability of the treated cells to move into the wound was their inability to move continuously. Time lapse movies showed that untreated control cells extended lamellipodia, stretched in the direction of the wound, and then retracted their tails causing them to move in a forward direction (supplemental Movie 1). The drug-treated cells also extended lamellipodia and polarized in the direction of the wound, but their tails appeared to have difficulty releasing from the dish and moving forward (supplemental Movie 2).

High Drug Concentrations Produce Microtubule Fragments and Inhibit Mitosis—To explain the ability of MIs to inhibit mitosis, we turned our attention to the presence of microtubule fragments that we noted in cells treated with drug concentrations that inhibited cell division. For example, Fig. 1 shows that microtubule fragments were rare in untreated cells, but they became evident in cells treated with the minimum drug concentrations able to inhibit normal cell division (Fig. 1, C and F). Moreover, the proportion of fragmented microtubules increased as the drug concentration increased (Fig. 1, D and G). To further demonstrate the involvement of microtubule fragments in drug action, we compared the vinblastine dose responses for microtubule fragment generation in wild-type and mutant CHO cell lines characterized by changes in microtubule assembly that confer altered drug sensitivity (20). As shown in Fig. 4A, there was a dose-dependent increase in the percentage of wild-type cells with microtubule fragments at drug concentrations that were significantly higher than those needed to suppress microtubule dynamics. CV 2-8, an α -tubulin mutant that is about 2-fold resistant to vinblastine in a colony formation assay (7) required more drug to generate similar microtubule fragments, whereas Tax 5-6, an α -tubulin mutant that is about 2-fold more sensitive to vinblastine (8), required less drug. It, thus, appears that the ability of vinblastine to generate microtubule fragments is closely linked to its ability to inhibit cell division in both wild-type and mutant cell lines. To be certain that these drug effects are not restricted to CHO cells, we treated COS-7, MCF-7, and Ishikawa cells for 1 h with vinblastine at twice its IC_{50} concentration for each cell line and found similar microtubule fragments (supplemental Fig. S3). Thus, the drug effects on microtubule fragment formation are rapid and are not cell line-specific. Similar effects were also seen using other MIs such as nocodazole, colchicine, griseofulvin, podophyllotoxin, and maytansine (data not shown). We con-

Novel Action of Antimitotic Drugs

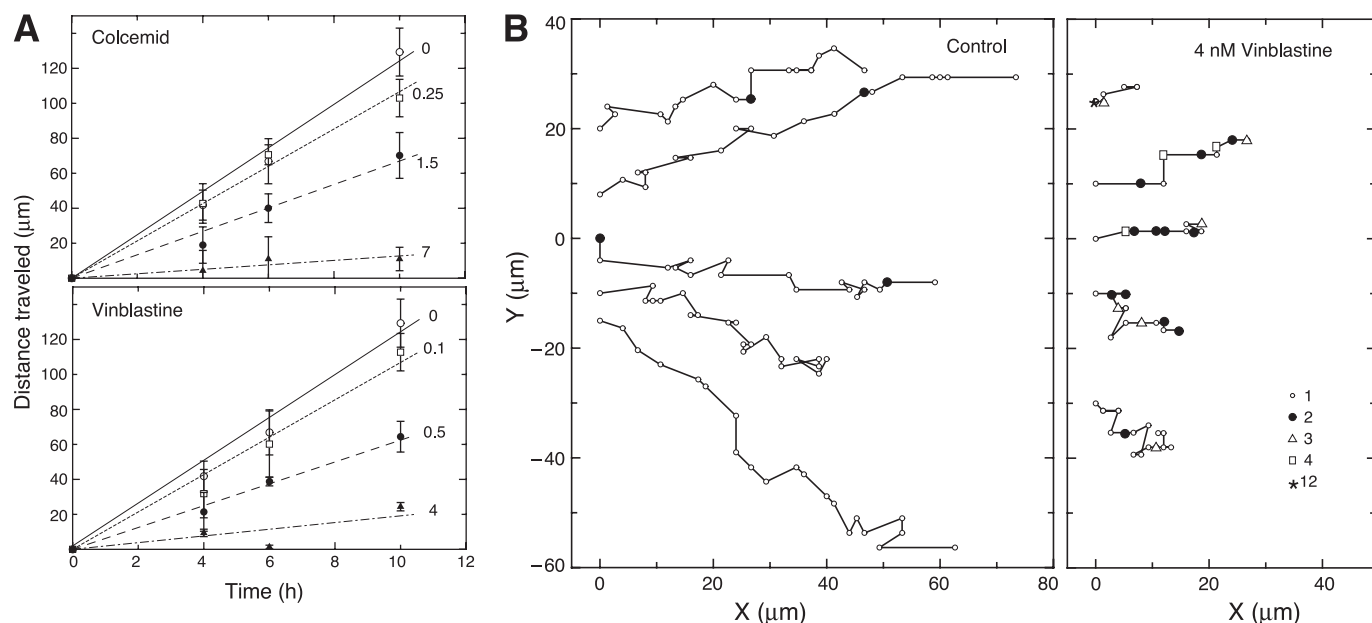


FIGURE 3. Effect of drugs on cell migration. *A*, CHO cells were treated with colcemid or vinblastine, and the distance they moved was measured using a wound healing assay. Each line is labeled with the nM drug concentration used in the experiment. Each data point and *error bar* represents the mean \pm S.D. of at least four independent experiments. *B*, control CHO cells or cells treated with 4 nM vinblastine were tracked while moving into a wound (situated toward the right). Each line represents a single cell. The *x* and *y* coordinates of the cell nucleus were measured every 15 min relative to a fixed position on the dish and plotted onto the graphs. Each *small open circle* represents a single 15-min time point. When movement did not occur after 15 min, the time points were assigned symbols according to the legend to indicate the number of 15-min intervals that passed before cell migration resumed. Thus, *filled circles* represent 2 intervals or 30 min, *open triangles* represent 3 intervals or 45 min, etc. Note that untreated cells exhibited few instances where they did not move in a 15-min time span, but vinblastine-treated cells had many such instances.

clude that most, if not all, drugs that inhibit microtubule assembly produce microtubule fragments in multiple mammalian cell lines.

To more clearly demonstrate the relationship between drug effects on microtubule assembly and cell behavior, we plotted cell division, cell migration, microtubule assembly, microtubule fragmentation, and microtubule dynamicity as a function of drug concentration (Fig. 4*B*). For cell migration, we plotted the normalized rates of cell movement into a wound derived from the slopes of the graphs shown in Fig. 3. For cell division, we plotted cell proliferation after 7 days of growth, but we also measured the percentage of cells that were multinucleated after 2 days and the mitotic index after overnight treatment, each of which gave very similar results (data not shown). Finally, we also plotted drug effects on the extent of microtubule assembly in the treated cells, measured as the percentage of total tubulin that was recovered by centrifugation of the microtubule cytoskeleton from a cell lysate. The results showed that drug effects on microtubule mediated functions are concentration-dependent. For both colcemid and vinblastine, low drug concentrations suppressed microtubule dynamicity and inhibited cell migration with similar dose-response relationships (Fig. 4*B*). In contrast, drug effects on cell division and microtubule assembly required significantly higher drug concentrations. The inhibition of cell division paralleled an increase in the percentage of cells with fragmented microtubules, suggesting that the two effects of drug action are linked. The decrease in microtubule assembly appeared to require a somewhat higher drug concentration. This could be due to the fact that we scored cells with relatively few (>10) microtubule fragments as positive but that much higher levels of fragmented microtubules might be

needed to have a significant impact on microtubule polymer levels. Alternatively, it might suggest that the drugs have an additional microtubule destabilizing activity at even higher drug concentrations. We concluded from these experiments that MIs likely inhibit cell migration by suppressing microtubule dynamics, but inhibition of cell division requires an additional action of the drugs that involves microtubule fragment formation. Whether this latter mechanism also affects microtubule assembly was less certain.

Fragments Are Formed by Microtubule Detachment from Centrosomes—In an effort to determine how microtubule fragments form, we examined EGFP-MAP4 transfected control and drug-treated cells by live cell imaging. Initially, we suspected that drug binding to tubulin might weaken interactions between subunits and thereby increase the frequency of lateral breaks in the microtubule wall; however, we found no evidence for this mechanism. Lateral breaks in microtubules were very rare in untreated cells (4 breaks in a total of 100 min of observation involving 20 cells) and were not seen to increase when the cells were treated with vinblastine at concentrations near the IC_{50} (3 lateral breaks under identical conditions). We also considered the possibility that microtubules were being nucleated in areas away from the centrosome, but we found no clear examples of this. Moreover, this mechanism would be expected to increase rather than decrease polymer levels in contradiction to the known action of these drugs.

In contrast to these other potential mechanisms for microtubule fragment generation, we noticed a significant increase of microtubule detachment from centrosomes at drug concentrations that produced microtubule fragments. Examples of microtubule detachment in untreated and vinblastine-treated

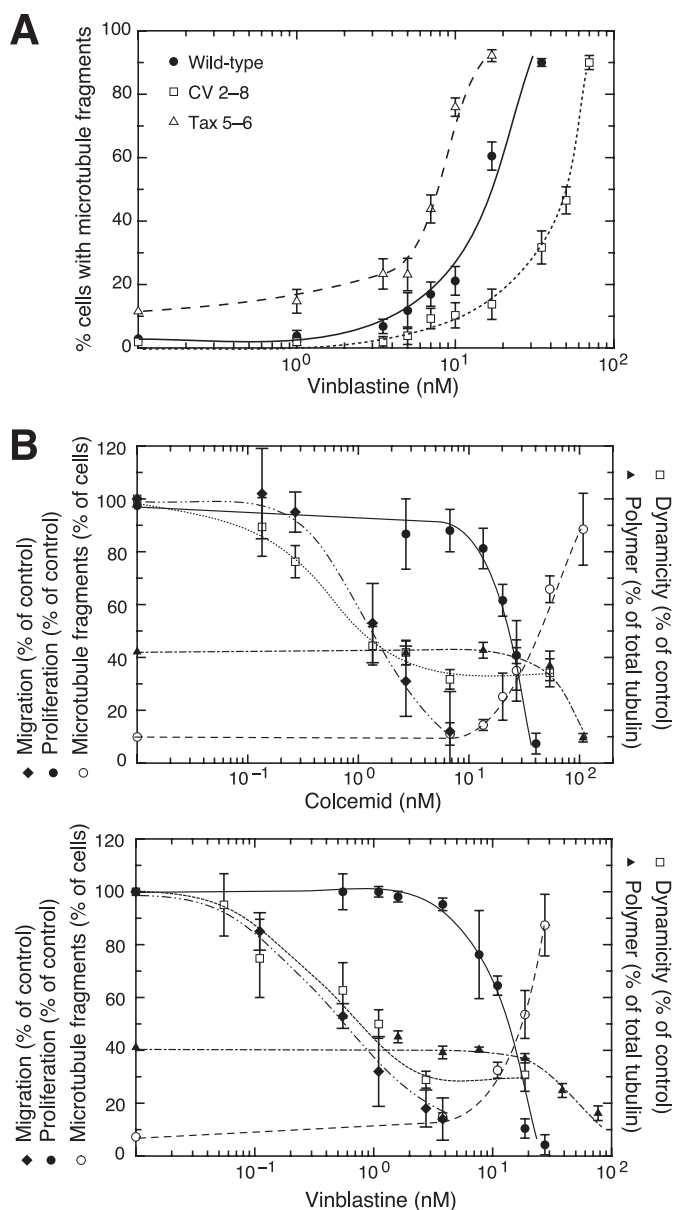


FIGURE 4. The appearance of microtubule fragments correlates with inhibition of cell division in wild-type and mutant CHO cells. *A*, wild-type cells, CV 2-8, a colcemid-resistant mutant that is also 2-fold resistant to vinblastine, and Tax 5-6, a paclitaxel-resistant mutant that is 2-fold more sensitive to vinblastine, were incubated in varying concentrations of vinblastine for 2 days and stained for tubulin immunofluorescence. The percentage of cells with >10 microtubule fragments was plotted against drug concentration for each cell line. *B*, cell proliferation (●) was measured using a clonogenic assay and expressed relative to untreated cells set at 100%. The percent of cells with >10 microtubule fragments (○) was counted after treating with colcemid or vinblastine at the indicated concentrations for 2 days. The rate of cell migration relative to untreated control cells (◆) was measured using a wound healing assay that began 30 min after adding the drug. Microtubule dynamicity (□) was calculated relative to untreated cells using the values found in supplemental Tables S1 and S2. The percent of total cellular tubulin found in microtubules (▲) was measured by lysing cells in a microtubule stabilizing buffer, centrifuging to separate polymerized from non-polymerized tubulin, and quantifying the tubulin in each fraction.

CHO cells are shown in Fig. 5. Detachment was infrequent in the non-treated control cells (0.17 ± 0.18 /cell/min) but increased ~ 9 -fold when the drug concentration reached a level that inhibited cell division (1.52 ± 0.45 /cell/min). It appeared that this microtubule release from centrosomes was a random

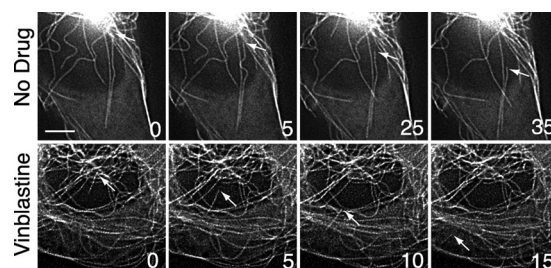


FIGURE 5. Microtubule detachment during interphase. CHO cells transfected with EGFP-MAP4 were left untreated (*upper panels*) or were treated 30 min with 15 nM vinblastine, the IC_{50} concentration for inhibition of cell division (*lower panels*). Fluorescence microscopic images, taken 5 s apart at 37 °C, were deconvolved to improve contrast. *Arrows* point to microtubule minus-ends before and after detachment. The numbers represent the time (in seconds) the images were taken relative to an arbitrary zero time point. *Bar* = 5 μ m.

event. Sometimes, detachment of long established microtubules was seen (see the *arrows* in the *upper panels* of Fig. 5), whereas other times newly nucleated microtubules were affected (see the *arrows* in the *lower panels* of Fig. 5). After detachment, microtubule fragments had varying lifetimes. Some depolymerized and disappeared rapidly, whereas others persisted with little or no changes in length for variable amounts of time. Some fragments remained near their site of detachment, whereas others translocated toward the cell periphery by an unknown mechanism. Although the free microtubule minus-ends generated by detachment were stable for varying lengths of time, shortening from this end was ultimately seen. It, therefore, appears likely that the released minus-ends lead to shorter microtubule lifespans and thereby contribute to the decrease in polymer induced by MIs. In agreement with a previous report, the free minus-end was never seen to elongate (21).

Spindle Microtubules Are More Dynamic and Detach More Frequently—Most of our experiments on drug-induced changes in microtubule behavior were carried out on interphase cells because the morphology of those cells facilitates measurements on individual microtubules. The ability of MIs to inhibit cell division, however, is mediated by their effects on microtubules during mitosis. To determine whether the changes we detected in microtubule behavior during interphase reflect similar changes that occur during mitosis, we measured the effects of vinblastine in prophase cells that remained relatively flat but could be clearly seen to have DNA condensation and separation of their spindle poles. Consistent with a previous study on mitotic microtubules (22), we found that prophase microtubule dynamics differed from interphase by having a 2-fold higher frequency of catastrophe and a 35% decrease in the time spent in pause leading to an overall 50% increase in dynamicity (Table 1). Compared with interphase (Fig. 2), prophase microtubule dynamics were characterized by more frequent growth and shortening events that were interrupted by short pauses (supplemental Fig. S4). Other parameters of dynamic instability including growth rates, shortening rates, and rescues were comparable between interphase and prophase. In addition to these commonly measured parameters of dynamic instability, we also noted that a higher fraction of the mitotic microtubules was dynamic. During interphase,

Novel Action of Antimitotic Drugs

~70% of the microtubules under observation appeared to have significant episodes of growth and shortening, whereas the remainder did not appreciably change during the period of observation. In the case of prophase cells, however, almost all the measurable astral microtubules appeared to be dynamic. Microtubules in the central spindle were too dense and bundled to be able to perform these measurements. The addition of 5 nM vinblastine, a concentration below what is needed to inhibit cell division, maximally suppressed prophase microtubule dynamics (Table 1 and supplemental Fig. S4). This observation confirms our earlier conclusion based on interphase microtubule behavior that suppression of dynamics is not sufficient to explain how MIs are able to inhibit mitosis.

Because vinblastine did not appear to inhibit cell division solely by its suppression of dynamic instability during mitosis, we measured microtubule detachment from spindle poles with and without drug treatment (Fig. 6A). Quantification of these events indicated that microtubules detach from spindle poles in prophase more frequently than they do from centrosomes during interphase (Fig. 6B). The addition of a low vinblastine con-

centration sufficient to inhibit dynamic instability behavior did not change the frequency of microtubule detachment, but a higher drug concentration capable of inhibiting cell division produced a significant increase in detachment in both interphase and prophase cells. Thus, we conclude that drug-mediated destabilization of microtubule attachment to spindle poles is involved in the inhibition of cell division.

To further determine whether similar drug concentrations affect both interphase and mitotic microtubules equally, we measured the formation of microtubule fragments in PtK2, a cell line that remains relatively flat during mitosis. As illustrated in supplemental Fig. S5A, mitotic cells frequently exhibited extensive microtubule fragmentation at vinblastine concentrations that had minimal effects on nearby interphase cells. To quantify this observation, we counted the percentage of mitotic *versus* the percentage of interphase cells that contained an elevated number of microtubule fragments at a series of drug concentrations (supplemental Fig. S5B). The results showed that mitotic microtubules were approximately two times more sensitive to vinblastine-induced fragment formation compared with interphase microtubules. Moreover, inhibition of cell division appeared to be in better agreement with the generation of microtubule fragments in mitotic rather than interphase cells. With the exception of this 2-fold shift in the dose-response curve, drug-induced changes in cytoplasmic microtubule behavior appeared to faithfully mirror the changes that occur during mitosis.

TABLE 1

Effect of vinblastine on microtubule dynamics in prophase CHO cells

Values shown represent the mean \pm S.E.

	Interphase		Prophase	
	0	0	5	35 nM
Growth				
Rate ($\mu\text{m}/\text{min}$)	16.2 \pm 0.8	17.1 \pm 1.6	9.9 \pm 0.7 ^a	12.3 \pm 1.0 ^a
Distance (μm)	3.2 \pm 0.4	2.5 \pm 0.3	0.9 \pm 0.1 ^a	1.3 \pm 0.1 ^a
Duration (sec)	12.2 \pm 1.2	9.0 \pm 0.6	5.4 \pm 0.3 ^a	6.4 \pm 0.3 ^a
Shortening				
Rate ($\mu\text{m}/\text{min}$)	28.2 \pm 2.3	24.6 \pm 2.0	13.5 \pm 1.5 ^a	13.9 \pm 0.9 ^a
Distance (μm)	5.2 \pm 0.6	3.3 \pm 0.4	1.4 \pm 0.1 ^a	1.6 \pm 0.1 ^a
Duration (sec)	11.2 \pm 1.1	8.7 \pm 0.9	6.3 \pm 0.3 ^a	6.7 \pm 0.3 ^a
% Time				
Growth	31.1 \pm 2.2	36.0 \pm 2.4	12.2 \pm 1.8 ^a	15.9 \pm 2.1 ^a
Shortening	21.1 \pm 1.9	33.0 \pm 2.8	14.0 \pm 0.8 ^a	16.3 \pm 1.7 ^a
Pause	47.8 \pm 3.1	31.0 \pm 3.9	73.8 \pm 3.9 ^a	67.7 \pm 3.3 ^a
Frequency (min^{-1})				
Catastrophe ^b	1.5 \pm 0.1	3.4 \pm 0.3	1.6 \pm 0.1 ^a	1.8 \pm 0.2 ^a
Rescue ^c	6.3 \pm 0.5	6.0 \pm 0.5	9.3 \pm 0.9 ^a	9.4 \pm 0.5 ^a
Dynamicity ^d ($\mu\text{m}/\text{min}$)	9.0 \pm 0.9	13.8 \pm 1.4	3.1 \pm 0.4 ^a	4.2 \pm 0.6 ^a
Number of microtubules	30	12	8	15

^a $p < 0.05$ compared to 0 concentration in prophase cells.

^b The transition from growth or pause to shortening.

^c The transition from shortening to growth or pause.

^d The total change of length per unit time of individual microtubules during their life histories.

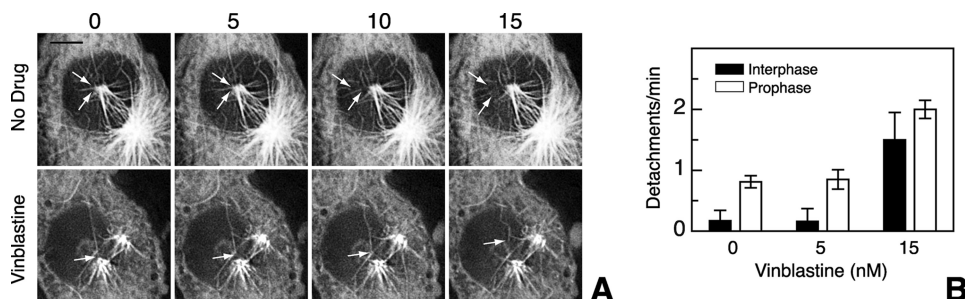


FIGURE 6. Microtubule detachment during mitosis. A, EGFP-MAP4-transfected CHO cells were left untreated (upper panels) or were treated 30 min with 15 nM vinblastine (lower panels) and were then viewed by live cell fluorescence microscopy. Prophase cells were located and photographed every 5 s. The images were deconvolved to improve contrast. Arrows point to the minus-ends of microtubules that detached from the spindle poles. Bar = 5 μm . B, the number of detachments seen in control- and drug-treated prophase and interphase cells were counted from captured images and divided by the total time of observation. The mean \pm S.D. was calculated from 11–20 cells during a total observation time of 50–80 min.

DISCUSSION

It is currently thought that MIs suppress microtubule dynamic instability and thereby inhibit mitosis as well as cell migration. However, some observations do not support this model. For example, MIs have been reported to inhibit cell migration at lower doses than those that are needed to inhibit mitosis (5, 23–25). In clonogenic assays for cell division, mutations in tubulin that confer resistance to vinca alkaloids make cells more sensitive to taxanes (7). Conversely, mutations that confer resistance to taxanes make cells more sensitive to vinca alkaloids (26). In addition, some tubulin mutations not only confer resistance to taxanes; they also make cell division dependent on the presence of taxanes (8, 27). These drug-dependent cells divide normally in the presence of taxanes, epothilones, and other agents that stabilize microtubules, but they are not rescued by vinca alkaloids, colchicine, or other agents that destabilize microtubules. Simple suppression of microtubule dynamics by all MIs cannot explain these observations, suggesting that MIs may act by at least two separate mechanisms.

In the studies described here, we report that low drug concentrations were able to suppress microtubule dynamics and inhibit cell migration, but they had no visible effect on the microtubule cytoskeleton or cell division. Low MI concentrations

have previously been reported to inhibit the migration of vascular endothelial cells, but this action was linked to an increase in microtubule dynamics as opposed to the suppression of dynamics that we observed in CHO cells (5, 28). This discrepancy likely results from differences in the two cell lines because similar low drug concentrations did not increase dynamics in A549 tumor cells (28). The mechanism by which modulation of microtubule dynamics inhibits cell migration is unknown. We observed that the main effect of vinblastine on the migration of CHO cells was to increase the amount of time in which the cells displayed no net movement. These cells extended lamellipodia toward a wound but appeared to have difficulty retracting their tails. This behavior could potentially be explained by a failure of the trailing end of the cell to detach from the dish, a possibility that is consistent with reports that microtubules are involved in the turnover of adhesion plaques (for review, see Ref. 3). Alternatively, suppressed dynamics could inhibit the ability of the microtubules to remodel themselves in the trailing end thereby resisting the forces that contract the tail (29). This latter mechanism is consistent with the demonstration that microtubule densification inhibits muscle contraction (30) and with reports that the more stable microtubules are found at the leading edge of migrating cells, whereas the more dynamic microtubules are at the trailing edge⁴ (31).

The higher drug concentrations needed to inhibit mitosis produced an increase of microtubule fragments. The production of these fragments is likely to be an important aspect of drug action because their numbers increased at the same drug concentrations that inhibited wild-type cell division and because the concentrations of drug needed for their production were shifted in mutant cell lines whose ability to divide was resistant or more sensitive to the drugs. The ability of MIs to produce microtubule fragments is not CHO- or drug-specific because fragments were seen in a variety of cell lines using multiple microtubule inhibitory drugs. Fragments were seen to arise from a drug-induced increase in microtubule detachment from the centrosomal area of the cell. Detachment or release of microtubules from centrosomes is a natural cellular process that was previously reported in PtK1 and L929 cells (21, 32). Noncentrosomal microtubules have also been observed in nerve (33), muscle (34), and epithelial cells (35), but the mechanism by which they form has not been defined and could well differ from the process that we observe. In interphase CHO cells, microtubule detachment is a rare event with a frequency (0.17/cell/min) that is intermediate compared with newt lung cells (0.02/cell/min) and PtK1 cells (1.5/cell/min) (21, 36). The reason for the variable frequencies is not clear, but they could reflect differences among cell lines or differences in the methods used to measure detachments. Our experiments indicate for the first time that the detachment rate increases dramatically when cells are treated with vinblastine concentrations sufficient to inhibit mitosis. Other recent studies indicate that tubulin mutations that create paclitaxel-dependent cells also dramatically increase the rate of microtubule detachment and that paclitaxel is able to inhibit this process at the same concentrations that rescue mutant cell division.⁴ Thus, in contrast to suppression of microtubule dynamics that occurs when cells are treated with low concentrations of all microtubule targeted

drugs, microtubule detachment is only affected by higher drug concentrations that may cause an increase or decrease in detachment depending on whether the drug inhibits or promotes microtubule assembly. The action of these drugs on microtubule detachment has not previously been described and needs to be taken into account when interpreting drug effects on living cells.

The mechanism by which microtubules detach from centrosomes is not known. At the present level of resolution, it cannot be determined whether the process involves disruption of the nucleating complex at the centrosome or lateral breaks in the centrosomal area. Centrosome fragmentation has been associated with a high rate of microtubule release from spindle poles during anaphase in LLPC1 cells (37), but this process is likely to be restricted to the latter stages of mitosis. We have not detected centrosome fragmentation during interphase or during prophase in either control or drug-treated CHO cells. Preliminary experiments to detect components of the centrosome such as γ -tubulin and pericentrin on newly detached microtubules have also been unsuccessful. This together with the observation that nucleation rates are similar in control and drug-treated cells⁴ leads us to conclude that the nucleation machinery remains largely intact in the presence of MIs. We, therefore, favor a mechanism in which microtubules are severed or destabilized by one or more proteins that localize predominantly to the centrosome. In such a mechanism, structural defects in the microtubule wall induced by drug binding could potentially make the microtubules more susceptible to these severing or destabilizing proteins. Although we cannot rule out the possibility that these structural defects could also make the microtubules more susceptible to mechanical breakage, the fact that we do not see appreciable breakage away from the centrosomal area makes this possibility less likely.

The low rate of microtubule detachment during interphase coupled with its activation in prophase suggests that it is primarily important during mitosis. This view is consistent with the fact that the drugs that affect this process block cell division. One possible role for microtubule detachment is that it could be required for the rapid remodeling of cytoplasmic microtubules into spindle microtubules during prophase. A second possibility is that detachment may contribute to the overall turnover of microtubules, which is known to increase during mitosis (38). A similar role for microtubule release in the turnover of cytoplasmic microtubules during interphase was previously proposed (21). A third more intriguing possibility, however, is suggested by electron microscopic studies that tracked microtubules through successive serial sections of mitotic spindles and concluded that as many as 50% of the microtubules were fragments with no attachment to the spindle poles (39) and by live cell studies showing that microtubule fragments become incorporated into the mitotic spindle (40). More recently it was reported that meiotic spindles also contain a large number of microtubule fragments and that these fragments may be necessary for increasing the density of microtubules in the central spindle (41, 42). This has led to a model in which spindles are composed of an overlapping "tiled array" of microtubule fragments held together by microtubule motor proteins (43). Based

Novel Action of Antimitotic Drugs

on these observations, we speculate that normal spindle function may depend on having a correct balance between attached and non-attached microtubules. MIs such as vinblastine and colcemid may be toxic because they shift the balance by greatly increasing the ratio between non-attached fragments and the longer, centrosome-anchored microtubules. Paclitaxel and epothilones may be toxic because they shift the balance toward too few non-attached fragments.

In summary, we have shown that MIs produce distinct effects at different concentrations. At low, subtoxic drug concentrations, they suppress plus-end microtubule behavior as well as most of the parameters associated with dynamic instability. As a consequence of this suppression, microtubules become more static and less able to remodel in response to demands imposed by changes in cell shape as occur, for example, during cell migration. At higher concentrations, MIs produce microtubule fragments by destabilizing microtubule minus-end attachment to centrosomes and spindle poles. Concomitant with the appearance of these fragments, mitosis is inhibited, but in agreement with previous reports, cytoplasmic microtubule polymer levels are not significantly affected (4). Major decreases in polymer levels occur only after MI concentrations reach even higher levels, suggesting that further binding of the drugs may be necessary to lower the steady state concentration of the microtubule polymer and arguing that it is the microtubule detachment from spindle poles rather than a change in polymer content that accounts for inhibition of mitosis. To rule out the possibility that mitotic microtubules are more sensitive to drug-induced depolymerization, we directly measured microtubule polymer in synchronized mitotic cells treated with colcemid or vinblastine and found no significant differences compared with unsynchronized cell populations (data not shown). Thus, our studies implicate microtubule detachment in the ability of drugs to perturb normal mitotic progression.

Acknowledgments—We are grateful to Dr. Joanne Olmsted for providing the EGFP-MAP4 plasmid used in these studies and to Dr. Xiangwei He for generously allowing us to use his DeltaVision microscope.

REFERENCES

1. Mitchison, T., and Kirschner, M. W. (1984) *Nature* **312**, 237–242
2. Goldman, R. D. (1971) *J. Cell Biol.* **51**, 752–762
3. Small, J. V., Geiger, B., Kaverina, I., and Bershadsky, A. (2002) *Nat. Rev. Mol. Cell Biol.* **3**, 957–964
4. Jordan, M. A., and Wilson, L. (2004) *Nature Reviews* **4**, 253–265
5. Pourroy, B., Honoré, S., Pasquier, E., Bourgarel-Rey, V., Kruczynski, A., Briand, C., and Braguer, D. (2006) *Cancer Res.* **66**, 3256–3263
6. Schwartz, E. L. (2009) *Clin. Cancer Res.* **15**, 2594–2601
7. Hari, M., Wang, Y., Veeraraghavan, S., and Cabral, F. (2003) *Mol. Cancer Ther.* **2**, 597–605
8. Schibler, M. J., and Cabral, F. (1986) *J. Cell Biol.* **102**, 1522–1531
9. Cabral, F., Sobel, M. E., and Gottesman, M. M. (1980) *Cell* **20**, 29–36
10. Yang, H., and Cabral, F. (2007) *J. Biol. Chem.* **282**, 27058–27066
11. Olson, K. R., McIntosh, J. R., and Olmsted, J. B. (1995) *J. Cell Biol.* **130**, 639–650
12. Minotti, A. M., Barlow, S. B., and Cabral, F. (1991) *J. Biol. Chem.* **266**, 3987–3994
13. Abraham, I., Marcus, M., Cabral, F., and Gottesman, M. M. (1983) *J. Cell Biol.* **97**, 1055–1061
14. Cabral, F., and Barlow, S. B. (1991) *Pharmacol. Ther.* **52**, 159–171
15. Kung, A. L., Sherwood, S. W., and Schimke, R. T. (1990) *Proc. Natl. Acad. Sci. U.S.A.* **87**, 9553–9557
16. Barlow, S., Gonzalez-Garay, M. L., West, R. R., Olmsted, J. B., and Cabral, F. (1994) *J. Cell Biol.* **126**, 1017–1029
17. Wang, X. M., Peloquin, J. G., Zhai, Y., Bulinski, J. C., and Borisy, G. G. (1996) *J. Cell Biol.* **132**, 345–357
18. Kamath, K., Wilson, L., Cabral, F., and Jordan, M. A. (2005) *J. Biol. Chem.* **280**, 12902–12907
19. Rhoads, D. S., and Guan, J. L. (2007) *Exp. Cell Res.* **313**, 3859–3867
20. Cabral, F. (2000) *Drug Resist. Updat.* **3**, 1–6
21. Keating, T. J., Peloquin, J. G., Rodionov, V. I., Momcilovic, D., and Borisy, G. G. (1997) *Proc. Natl. Acad. Sci. U.S.A.* **94**, 5078–5083
22. Rusan, N. M., Fagerstrom, C. J., Yvon, A. M., and Wadsworth, P. (2001) *Mol. Biol. Cell* **12**, 971–980
23. Liao, G., Nagasaki, T., and Gundersen, G. G. (1995) *J. Cell Sci.* **108**, 3473–3483
24. Vacca, A., Iurlaro, M., Ribatti, D., Minischetti, M., Nico, B., Ria, R., Pellegrino, A., and Dammacco, F. (1999) *Blood* **94**, 4143–4155
25. Hotchkiss, K. A., Ashton, A. W., Mahmood, R., Russell, R. G., Sparano, J. A., and Schwartz, E. L. (2002) *Mol. Cancer Ther.* **1**, 1191–1200
26. Yin, S., Bhattacharya, R., and Cabral, F. (2010) *Mol. Cancer Ther.* **9**, 327–335
27. Cabral, F. R. (1983) *J. Cell Biol.* **97**, 22–29
28. Pasquier, E., Honoré, S., Pourroy, B., Jordan, M. A., Lehmann, M., Briand, C., and Braguer, D. (2005) *Cancer Res.* **65**, 2433–2440
29. Brangwynne, C. P., MacKintosh, F. C., Kumar, S., Geisse, N. A., Talbot, J., Mahadevan, L., Parker, K. K., Ingber, D. E., and Weitz, D. A. (2006) *J. Cell Biol.* **173**, 733–741
30. Cheng, G., Zile, M. R., Takahashi, M., Baicu, C. F., Bonnema, D. D., Cabral, F., Menick, D. R., and Cooper, G., 4th (2008) *Am. J. Physiol. Heart Circ. Physiol.* **294**, H2231–H2241
31. Salaycik, K. J., Fagerstrom, C. J., Murthy, K., Tulu, U. S., and Wadsworth, P. (2005) *J. Cell Sci.* **118**, 4113–4122
32. Abal, M., Piel, M., Bouckson-Castaing, V., Mogensen, M., Sibarita, J. B., and Bornens, M. (2002) *J. Cell Biol.* **159**, 731–737
33. Ahmad, F. J., and Baas, P. W. (1995) *J. Cell Sci.* **108**, 2761–2769
34. Tassin, A. M., Maro, B., and Bornens, M. (1985) *J. Cell Biol.* **100**, 35–46
35. Bacallao, R., Antony, C., Dotti, C., Karsenti, E., Stelzer, E. H., and Simons, K. (1989) *J. Cell Biol.* **109**, 2817–2832
36. Waterman-Storer, C. M., and Salmon, E. D. (1997) *J. Cell Biol.* **139**, 417–434
37. Rusan, N. M., and Wadsworth, P. (2005) *J. Cell Biol.* **168**, 21–28
38. Saxton, W. M., Stemple, D. L., Leslie, R. J., Salmon, E. D., Zavortink, M., and McIntosh, J. R. (1984) *J. Cell Biol.* **99**, 2175–2186
39. Mastronarde, D. N., McDonald, K. L., Ding, R., and McIntosh, J. R. (1993) *J. Cell Biol.* **123**, 1475–1489
40. Tulu, U. S., Rusan, N. M., and Wadsworth, P. (2003) *Curr. Biol.* **13**, 1894–1899
41. Burbank, K. S., Groen, A. C., Perlman, Z. E., Fisher, D. S., and Mitchison, T. J. (2006) *J. Cell Biol.* **175**, 369–375
42. Srayko, M., O’toole, E. T., Hyman, A. A., and Müller-Reichert, T. (2006) *Curr. Biol.* **16**, 1944–1949
43. Yang, G., Houghtaling, B. R., Gaetz, J., Liu, J. Z., Danuser, G., and Kapoor, T. M. (2007) *Nat. Cell Biol.* **9**, 1233–1242